Non-destructive depth-dependent morphological characterization of ferroelectric:semiconducting polymer blend films

Nicoletta Spampinato, Gilles Pecastaings, Mario Maglione, Eleni Pavlopoulou, Georges Hadziioannou

Original Contribution

Non-destructive depth-dependent morphological characterization of ferroelectric:semiconducting polymer blend films

N. Spampinato,[a] G. Pecastaing,[a] M. Maglione,[b] G. Hadziioannou,[a] E. Pavlopoulou[a,c,*]

[a] Bordeaux INP, Université de Bordeaux, CNRS, LCPO - UMR 5629, 16 Av. Pey-Berland, 33607, Pessac, France

[b] Institut de Chimie de la Matiere Condensée de Bordeaux, (ICMCB-UPR9048), CNRS, 87 Av. Dr Schweitzer, 33608, Pessac, France

[c] Institute of Electronic Structure and Laser (IESL), Foundation for Research and Technology – Hellas (FORTH), Vassilika Vouton, 71110, Heraklion, Greece

[*] Corresponding author.
E-mail address: epavlopoulou@enscbp.fr (E. Pavlopoulou).

ORCID numbers:
N. Spampinato:
G. Pecastaings: 0000-0002-9109-6225
M. Maglione: 0000-0002-5747-8879
G. Hadziioannou: 0000-0002-7377-6040
E. Pavlopoulou: 0000-0002-5291-0132

Abstract

Herein we investigate the technologically relevant blend of the ferroelectric polymer poly(vinylidene fluoride-co-trifluoroethylene), P(VDF-*co*-TrFE), with the semiconducting polymer poly(3-hexylthiophene), P3HT, by means of a combination of Scanning Probe Microscopy techniques, namely Atomic Force Microscopy, Conductive Force Microscopy, Kelvin Probe Force Microscopy and Piezoresponse Force Microscopy. This combination proves to be a powerful tool for the non-destructive morphological reconstruction of multi-functional nano-structured thin films, as those under study. Each modality allows discerning the two blend constituents based on their functionality, and, additionally, probes layers of different thickness with respect to the films surface. The depth-dependent information that is collected allows a qualitative reconstruction of the blend's composition and morphology both in-plane and out-of-plane of the film. We demonstrate that P3HT exhibits the tendency to reside the film surface at an almost constant composition of 15%, independent of blend's composition. Increasing the P3HT content in the blend results in the segregation of P3HT at the upper layers of the films, partially buried below a P(VDF-co-TrFE) superficial layer. The depletion of P3HT from the substrate/film interface is reflected by the poor existence of conducting pathways that connect the top and bottom planes of the film. The three-dimensional morphology of this polymer blend that is revealed thanks to the employed techniques deviates substantially from the ideal morphology proposed for the efficient performance of the targeted memory devices.

Keywords

P(VDF-co-TrFE), P3HT, polymer blends, scanning probe microscopy, morphology, non-volatile memories

Declarations

Funding (information that explains whether and by whom the research was supported)
The authors acknowledge receiving funding from the Labex AMADEus (ANR-10-LABEX-0042-AMADEUS) and the French state Initiative d'Excellence IdEx (ANR-10-IDEX-003-02). Financial support from the HOMERIC Industrial Chair (Arkema/ANR) with the grant agreement no AC-2013-365 is also acknowledged.

Conflicts of interest/Competing interests
The authors declare no conflict of interest.

Availability of data and material (data transparency)
Not applicable

Code availability (software application or custom code)
Not applicable

1. Introduction

The advance of organic electronics continuously pushes research efforts towards multi-functionality, often achieved by combining in the same device different functional materials. Devices that incorporate polymer blends as the active layers constitute such an example. In particular, blends of ferroelectric, FE, and semiconducting, SC, polymers have been proposed as efficient active layers for non-volatile memory devices.[1] Thanks to their bistable reversible polarization, ferroelectrics are appropriate materials for memories. However, capacitors that incorporate pure ferroelectric layers suffer from destructive read-out, since reading requires the application of an electric field that exceeds the coercive field, E_c.[2,3] The introduction of a semiconducting phase is necessary in order to induce the non-destructive read-out of the programmed state.[1] In order to combine the ferroelectric with the semiconducting functionality within the same active layer and demonstrate a performing non-volatile memory, lateral heterostructures have been successfully employed. In a lateral heterostructure, the ferroelectric and the semiconducting phases are arranged side-by-side, forming domains that are perpendicular to the device plane and continuously connect the top to the bottom electrode.[4] Ideally, the ferroelectric material should form a matrix in which the semiconducting material is embedded, forming domains/columns that expand through the entire thickness of the matrix film, providing the necessary continuous conducting pathways.[5,6,4] This specific morphology is critical for the operation of the memory device, since the operation mechanism relies on the formation of clear interfaces between the two constituents and the metal electrodes. Specifically, according to current understanding,[7,8] holes accumulate along the semiconducting/ferroelectric interface. Polarization of the ferroelectric matrix induces a strong stray field locally between the semiconducting-ferroelectric interface and the metal electrode, which results in a reduced depletion width in the semiconductor and subsequent charge injection by tunneling from the anode to the semiconducting phase. Therefore, ferroelectric polarization is used to control the injection barrier locally at the semiconductor/metal interface, switch the resistance of the diode that is practically formed by the metal/semiconductor/metal sequence and, finally, control charge flow via the semiconducting phase.[1,4] In practice, these ferroelectrically-driven diodes operate as vertical (with respect to the device's plane) field-effect transistors at the pinch-off.[7]

These lateral heterostructures have been traditionally prepared by phase-separated blends of a ferroelectric and a semiconducting polymer. Poly(vinylidene fluoride-co-trifluoroethylene), P(VDF-co-TrFE), has been used as the ferroelectric polymer[9-12] while poly(3-hexylthiophene), P3HT, poly[3-(ethyl-5-pentanoate) thiophene-2,5-diyl] (P3EPT),[13] poly(9,9-dioctylfluorenyl-2,7-diyl) (PFO),[10] or poly[(9,9-din-octylfluorenyl-2,7-diyl)-alt-(benzo[2,1,3]thiadiazol-4,8-diyl)](F8BT)[13,14] have been employed as the semiconducting component. Given the crucial role of morphology in memories operation and driven by the need for performance improvement, several studies appeared in literature investigating the morphology of the P(VDF-co-TrFE):P3HT blend. In 2008 Asadi *et al.* claimed the formation of a phase-separated columnar-like network that comprises P3HT columns embedded in the ferroelectric matrix, with a typical lateral phase separation length of around 200 nm.[1] In 2010 McNeill, Asadi and co-workers[5] utilized AFM and Scanning Transmission X-ray Microscopy (STXM) to show that the two polymers form a phase-separated structure, where semiconducting columns with a lateral size ranging from 100 nm to 500 nm depending on the ferroelectric:semiconducting ratio, are extended through the entire thickness of P(VDF-co-TrFE):P3HT blend thin films. Even though STXM allows investigating the bulk structure of thin polymeric films[15] the authors

underlined that one needs to “be careful in reading too much the vertical information and the appearance of a wetting layer at the interface demands for further investigations with surface-sensitive techniques”. Khikhlovskyi *et al.* used atomic force microscopy (AFM) to show that the semiconducting polymer domains can form either convex protrusions at the film surface, or concave depressions, these latter being mainly responsible for the charge conduction in the device.[13] In order to reconstruct the three dimensional blend morphology, they selectively dissolved the different components and revealed the existence of various types of embedded semiconductor domains as well as a thin wetting layer at the bottom electrode. Semiconducting domains that go through the entire film thickness and serve to connect the bottom and top electrodes were observed, while others were electrically non-active, either protruding at the surface (not connected with the bottom electrode) or laying on the substrate, reminiscent of a partial wetting layer buried by the matrix.[14] However, such “electrically blind” domains are undesirable for device operation because they do not contribute to the overall current and could even be detrimental for device performance by either inhibiting charge injection at the anode-semiconducting interface, or charge collection by the cathode.[15] Yet, the destructive approach followed by these authors can result in partial information regarding the spatial distribution of one phase with respect to the other.

Driven by the need to provide an integrated and realistic picture of the complex morphology of these blends, and in view of the technological interest that these lateral heterostructures can have in emerging applications such as MEMOLEDS, artificial synapses, or thermistors,[4] we herein present a qualitative study of the three-dimensional morphology of P(VDF-co-TrFE):P3HT blends, employing non-destructive techniques. Explicitly, a combination of different Scanning Probe Microscopy modalities has been utilized: Atomic Force Microscopy (AFM), Piezoresponse Force Microscopy (PFM), Kelvin Probe Force Microscopy (KPFM) and Conductive Atomic Force Microscopy (C-AFM). Each modality allows discerning the two blend constituents based on their functionality. Moreover, each modality probes a different layer of the film; AFM and PFM are purely surface sensitive techniques, KPFM has a sampling depth that goes over 100 nm when semiconducting materials are investigated, while C-AFM allows mapping the charge flow pathways that are continuous between the tip (i.e. the film surface) and the bottom electrode (i.e. the substrate/film interface). Therefore, morphological information on all three dimensions of the ferroelectric:semiconducting blend films can be qualitatively extracted by combining the above modalities, in a non-destructive way. By exploring the blend morphology with respect to blend composition, useful information on the physical reasons that drive morphology has been extracted. It is underlined that the present study uses P(VDF-co-TrFE):P3HT as a model system, yet the combination of the above modalities can be generalized as a powerful tool for the structural study of other complex multifunctional systems.

2. Materials and Methods

2.1. Materials and Samples preparation

The statistical copolymer P(VDF-co-TrFE) (with a 75/25 VDF/TrFE molar ratio and a M_w of 400 kDa) was provided by courtesy of Piezotech® FC (France). Regio-regular P3HT, rr-P3HT, with a M_w of 60 kDa and a

regioregularity of 96 % was synthesised in our Laboratory according to Grignard metathesis method. Tetrahydrofuran, THF, (SIGMA-Aldrich) was used as received without any further purification.

Note that most of the studies on P(VDF-co-TrFE):P3HT blends utilize regio-irregular P3HT, rir-P3HT, which ensures better solubility of P3HT in THF and easier film formation. However, this choice leads to amorphous semiconducting ~~SC~~ domains. Herein we opt to utilize regio-regular P3HT that leads to the formation of semi-crystalline P3HT domains. In fact, semi-crystalline P3HT is known to allow better charge conduction than the amorphous one, which is extremely important for efficient charge transport in electronic devices. Holes mobility in rr-P3Ht is reported to be an order of magnitude higher than that in rir-P3HT ($\mu_{h+\text{rr-P3HT}} = 10^{-3}$ cm² V^{-1} s^{-1}, $\mu_{h+\text{rir-P3HT}} = 10^{-4}$ cm² V^{-1} s^{-1}),[16] thanks to the ordered π-π stacking of the thiophene rings obtained through the crystallization of the polymer. The use and study of rr-P3HT-containing blends is therefore preferable with respect to rir-P3HT-containing ones, since the final goal is their incorporation as active layers in organic electronic devices.

P(VDF-co-TrFE) and rr-P3HT were co-dissolved in THF at a total concentration of 25 mg mL^{-1}. Three weight ratios of P(VDF-co-TrFE):rr-P3HT have been prepared, i.e. 95:5 $_{wt/wt}$, 90:10 $_{wt/wt}$ and 80:20 $_{wt/wt}$ and spin-coated onto cleaned ITO substrates.

Films with a thickness of ≈ 250 nm were obtained, as measured by profilometry (BRUKER DEKTAK XT-A). The films have been annealed on a precision hot stage from RT to 135 °C and an isothermal step has been performed for 15 min in order to increase both polymers crystallinity[17] and promote phase separation. Then the films were let to cool down slowly until RT on the same hot stage.

2.2. Characterizations

Atomic force microscopy (AFM Dimension FastScan, Bruker) was used in tapping mode to characterize the surface morphology of the films. Silicon cantilevers (Fastscan-A) with a typical tip radius of ≈ 5 nm, a spring constant of 18 N m^{-1} and a cantilever resonance frequency of about 1.4 MHz were used.

Conducting AFM (C-AFM) measurements were performed in PeakForce mode with a Dimension ICON (Bruker) equipped with a TUNA module. Platinum–iridium-coated probes (SCM-PIT, Bruker) with a spring constant of 2.8 N m^{-1} and resonant frequency of 75 kHz were used. For C-AFM measurements, a DC bias of 5 V was applied between the bottom electrode and the tip.

Kelvin probe force microscopy (KPFM) measurements were performed in ambient atmosphere with a Dimension ICON (Bruker) in frequency–modulated mode (58 kHz, scan rate of 1 Hz, tip velocity of 10 μm sec^{-1}, drive amplitude 4 V). Highly doped Si probes (PFQNE-AL, Bruker) were used.

For Piezoresponse force microscopy (PFM) measurements, Platinum–iridium-coated probes (SCM-PIC, Bruker) with a spring constant of 0.2 N m^{-1} and resonant frequency of 15 kHz were used. The applied voltage is 4 V.

Contact angle measurements were carried out at room temperature with a Kruss ADVANCE goniometer (Kruss Drop Shape Analyzer DSA100), by means of the sessile drop method. For this analysis three liquids were

used: water, ethylene glycol and diiodomethane. A droplet having about 1 μL of each liquid probe is deposited by a syringe on dry P(VDF-co-TrFE) and P3HT films, 250nm thick, which have been deposited on ITO substrates and have been annealed in the same way as the blend herein studied (135°C for 15 minutes). Static contact angles values were detected immediately after the sessile drop formation on the film surface, waiting for the drop to stabilize. For each liquid at least three measurements have been taken into account in consistency to the protocols applied for the OWRK model.[18] The surface tensions of P(VDF-co-TrFE) and P3HT have been calculated by means of the Kruss ADVANCE software, via the construction of the wetting envelope plot and the application of the OWRK model.[19]

3. Results and Discussion

Initial structural characterization of the film surface has been performed using PFM. This is a contact mode imaging technique that allows recording the electromechanical response of a material, in our case of the piezoelectric and ferroelectric P(VDF-co-TrFE). During scanning, an AC voltage is applied between the tip and the sample. The ITO, on top of which the film has been deposited, represents the ground contact, while the PFM conductive probing tip acts as the top electrode. If the electrically stimulated film is piezoelectric, expansions and contractions will be recorded as a vertical mechanical displacement that exhibits both an amplitude and a phase component (VPFM amplitude and VPFM phase images). The amplitude of the mechanical displacement vertical to the substrate's plane gives information about the magnitude of the electromechanical polarization displacement. The sample piezoresponse amplitude, directly measured with the help of the reflected laser beam and the photodetector, whose signal is represented in Volts, was calibrated in nanometers using the cantilever deflection sensitivity (nm/V). For this study, we used the nominal deflection sensitivity of the SCM-PIC probes (224 nm/V). The various orientations of the polarized piezoelectric domains are shown in the VPFM phase image. The height (topography) image along with the VPFM amplitude and VPFM phase images are recorded simultaneously during scanning, and correspond to the same sample area.

In Figure 1 the PFM height images (Figures 1a, 1d, 1g) and the corresponding VPFM amplitude images (Figures 1b, 1e and 1h) and VPFM phase images (Figures 1c, 1f and 1i) are shown for ~~a~~ samples with a P(VDF-co-TrFE):P3HT composition of 95:5 $_{wt/wt}$ (first row), 90:10 $_{wt/wt}$ (second row) and 80:20 $_{wt/wt}$ (third row). When electrical stress is applied to the film through the piezo-tip a mechanical response is recorded only from the piezoelectric P(VDF-co-TrFE) matrix (pink and blue regions in Figures 1b,1c, 1e, 1f, 1h and 1i).[16,20] The P3HT domains do not respond to the applied voltage as shown by the green regions, indicating absence of displacement, since P3HT is not piezoelectric. Thus, the piezoelectric and semiconducting phases that populate the surface of the film can be discriminated. In line with other studies of polymeric systems that comprise both ferroelectric and semiconducting phase in physical contact,[21-23] our PFM characterization demonstrates that P(VDF-co-TrFE) retains its piezoelectric functionality. Note that piezoelectric functionality can be lost due to depolarization induced by incomplete compensation of charges by the neighboring semiconducting phase.[24,25] This is already a very important outcome since the applications of this blend necessitates the retention of polarization by P(VDF-co-TrFE).

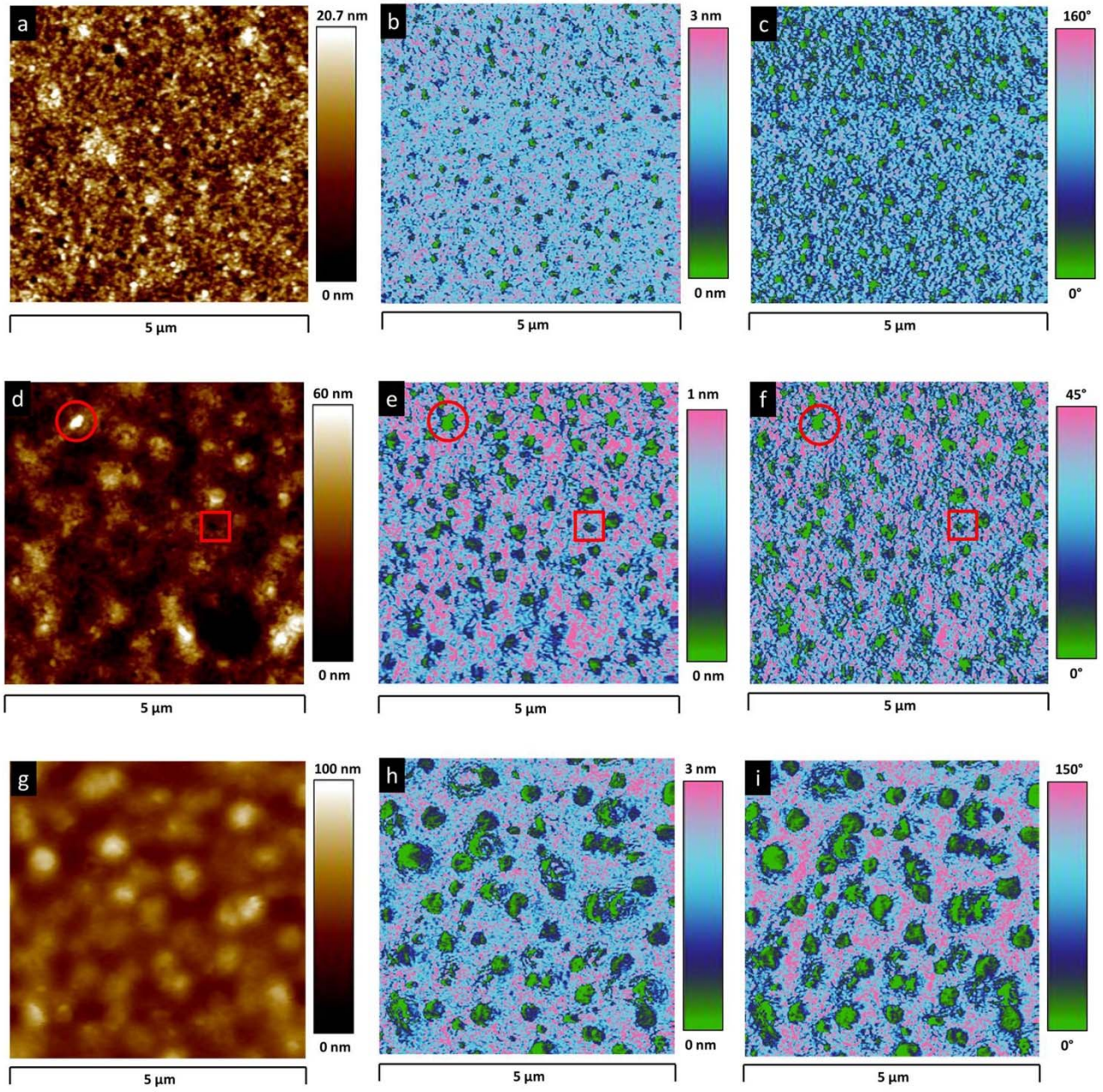

Figure 1 - *5 µm x 5 µm PFM height image, VPFM amplitude image and VPFM phase images recorded for the 95:5 $_{wt/wt}$ P(VDF-co-TrFE):rr-P3HT blend (a, b and c respectively), for the 90:10 $_{wt/wt}$ blend (d, e and f, respectively), and for the 80:20 $_{wt/wt}$ blend (g, h and i, respectively. All three images are recorded simultaneously on the same sample region. The circles and squares denoted on the three images of 90:10 $_{wt/wt}$ blend correspond to the same features. The red circle represents a convex P3HT domain, while the red square corresponds to a concave P3HT domain.*

These PFM images show that P3HT domains of irregular shapes exist at the surface of the ferroelectric matrix. In Figures 1d, 1e and 1f circles and squares are used to evidence two different morphological features, as they appear on the three different PFM images. By comparing Figure 1d and Figure 1e we see that both features correspond to P3HT. In Figure 1a the red circle denotes a superficial convex protrusion, while the

square corresponds to a superficial concave depression. The observation that semiconducting domains at the surface can be either convex or concave, appearing as protrusions or depressions has been already reported in previous works,[1,5,6] and demonstrates that AFM topography images is not a reliable way to study the surface morphology of this blend. From the PFM images we can estimate a rough P3HT domain size for the three different blend compositions. This domain size was estimated by averaging the rough diameter of all P3HT features that appear in the VPFM amplitude images. As the content of P3HT increases, the mean diameter of the semiconducting features increases as well, going from about 100 nm for the 95:5 $_{wt/wt}$ blend (Figure 1b), to 160 nm for the 90:10 $_{wt/wt}$ blend (Figure 1e), to 460 nm for the 80:20 $_{wt/wt}$ blend (Figure 1h). The associated standard deviations are comparable to the mean values. This increase in size qualitatively agrees with the increase in P3HT domain size reported based on quantitative analysis of AFM images,[6] but the absolute values we derive are half with respect to those derived by AFM for the same compositions. Additionally, PFM images witness a very big polydispersity in size. For sample 80:20 $_{wt/wt}$ in particular, big domains of the order of 800 nm coexist with small domains of the order of 50 nm. This result could be representative of a nucleation and growth type of phase separation and puts in question the AFM-derived outcome on the spinodal decomposition driven phase separation.[6] We underline that the phase separation of P(VDF-co-TrFE) and P3HT is assisted and enhanced by the natural tendency of these polymers to crystallize. Even in case of regio-irregular P3HT, the crystallization of the P(VDF-co-TrFE) matrix probably dominates the physical processes that drive the resulting blend morphology, and therefore, should not be omitted.

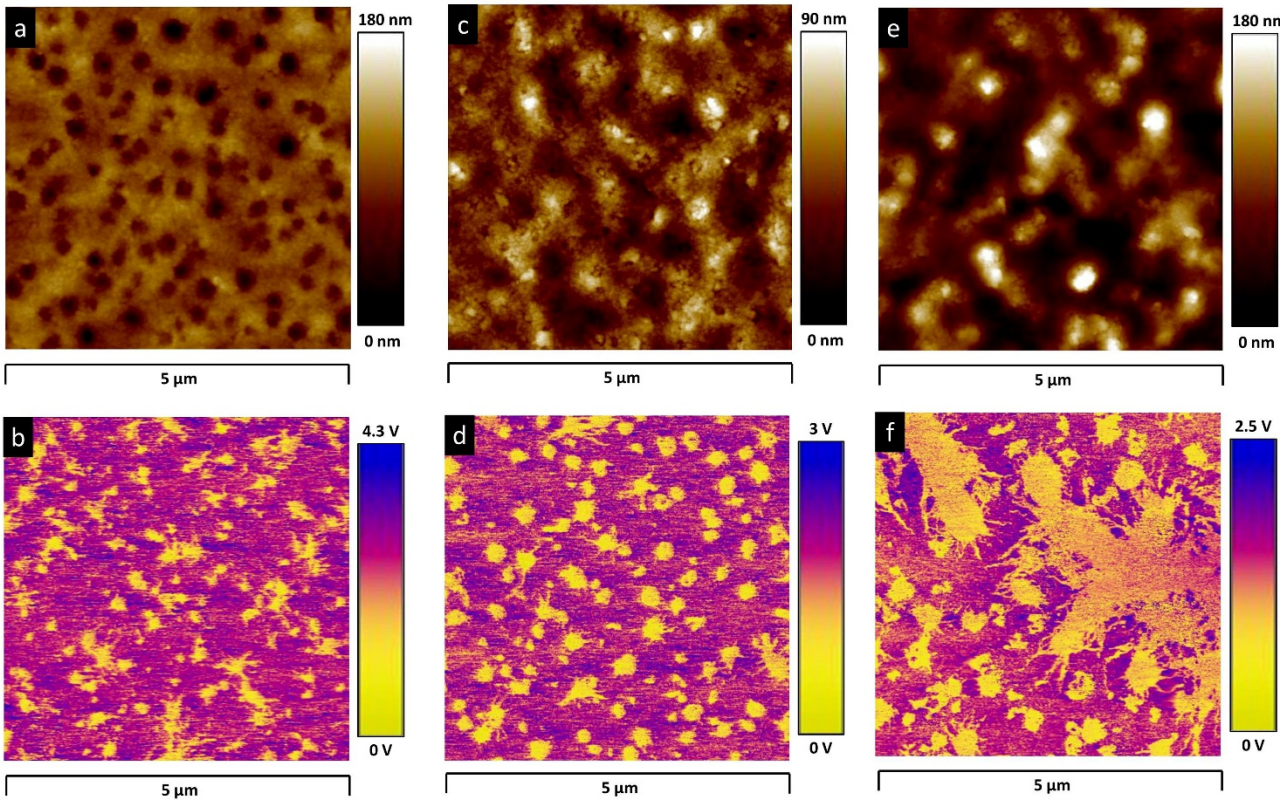

Figure 2 - *KPFM topography images (top row) and the corresponding surface potential maps (bottom row) for the following compositions of the P(VDF-co-TrFE):P3HT blends: 95:5 $_{wt/wt}$ (a and b), 90:10 $_{wt/wt}$ (c and d), and 80:20 $_{wt/wt}$ (e and f).*

The correlation between the topographic and electronic properties of the three blends has been investigated by means of KPFM. KPFM enables discriminating two polymers that demonstrate different electronic behavior by providing the surface potential map of the sample under study at the nanoscale. The potential measured between the tip and the surface of the film is called contact potential difference, V_{CPD},[26] and is defined as follows:

$$V_{CPD} = \frac{\Phi_{tip} - \Phi_{sample}}{-e} \quad (1)$$

where Φ_{sample} and Φ_{tip} are the work functions of the sample and the tip respectively, and e is the electronic charge. When the tip is brought close to the film surface, an electrical force is generated between the tip and the surface, due to the differences in their Fermi energy levels.[26] Therefore, regions where a larger V_{CPD} is recorded correspond to an electrical insulator; *vice versa* when the measured V_{CPD} is low, a semiconducting material is detected. It is underlined that KPFM, as opposed to AFM and PFM, is not a purely surface-sensitive technique,[27] but its sampling depth goes up to over 100 nm when semiconducting materials are investigated. Given that the thickness of the investigated films is 250 nm, the KPFM information recorded herein is coming from a thick layer at the upper part of the film, of almost half thickness with respect to the whole film. This suggests that KPFM exhibits a sort of ‘‘bulk sensitivity’’.

In Figure 2 the topography images (top row) and the corresponding surface potential maps (bottom row) are reported for the blends with a ferroelectric:semiconducting weight ratio of 95:5 $_{wt/wt}$ (Figures 2a and 2b respectively), 90:10 $_{wt/wt}$ (Figures 2c and 2d) and 80:20 $_{wt/wt}$ (Figures 2e and 2f). P3HT and P(VDF-co-TrFE) can be unambiguously discriminated on the surface potential maps. The yellow features represent regions with low Φ, namely the semiconducting P3HT, while the pink regions correspond to regions with high Φ, that is the insulating P(VDF-co-TrFE) matrix.

In consistence with the PFM results, KPFM images show that the mean P3HT domain size increases with increasing the P3HT content in the blends, retaining a significant polydispersity. Furthermore, the P3HT domains have the tendency to connect with each other, creating a network. This is witnessed by the presence of connecting P3HT lines between the P3HT domains, even at the lowest P3HT content (Figure 2b). These connecting lines expand when P3HT loading increases and result in big disordered domains for the 80:20 $_{wt/wt}$ blend, of the order of several μm in size (Figure 2f). The appearance of these interconnecting lines and their relation to the evolution of the morphology with increasing P3HT loading could be related to a nucleation and growth type of phase separation. In that scenario, P3HT domains appear in the ferroelectric matrix, probably driven not only by the different chemical composition of the two polymers but also by the tendency of P3HT to crystallize. Spin-coated P3HT is known to crystallize forming nanofibrils[28] and these nanofibrils grow by expanding along the fibers long axis. Therefore, the interconnecting lines we observe in KPFM images could be P3HT nanofibrils or bunches of them. Note that, as discussed above, a nucleation and growth driven phase separation is also implied by the domain size information estimated by analyzing the VPFM images.

The large P3HT domains are not apparent in the corresponding VPFM images. Recalling that KPFM probes a large thickness of the film while PFM probes the surface, we can conclude that a part of the P3HT domains that are apparent in the KPFM images is in fact buried below a P(VDF-co-TrFE) surface layer. Such an

arrangement of P3HT with respect to the electrodes (in other words, the decrease of direct contact area between the semiconductor and the electrode) is not desirable for the memory applications that primarily this blend targets, since the operation mechanism of the memories relies on the formation of interfaces where the ferroelectric phase, the semiconducting phase and the metal electrode coexist, as it was described in the Introduction. Moreover, the network-like P3HT distribution observed for the 20 wt% P3HT loading deviates significantly from the columnar structure that has been described as ideal for the operation of these memories. Hence, this KPFM study shows that the P3HT content in the blend should not exceed 10 wt%, so as to avoid the formation of the interconnected P3HT network and concurrently balance the amount of P3HT that resides at the surface, not buried by P(VDF-co-TrFE).

Moving further, we investigated the existence of semiconducting pathways that link the bottom to the top surface. For this, we performed Conductive Atomic Force Microscopy. In C-AFM the samples are grounded through the ITO bottom electrode, while the AFM tip serves as the top electrode. Topography and high-resolution electric current flow maps (in the range of 2 pA to 1 μA) are simultaneously measured in Tunneling AFM (TUNA) mode and PeakForce TUNA™ mode, at the contact point of the tip with the surface of the sample. Variations of electrical conductivity across medium- to low-conducting and semiconducting materials are mapped. If a current flow is passing between the bottom electrode and the AFM tip, it will be recorded. Therefore with C-AFM we are able to study the existence of P3HT domains that traverse the film perpendicularly to its plane, *i.e.* along the entire film thickness, and thus gain insight in the spatial distribution of the semiconducting phase in all three dimensions. Topography images (top row of Figure 3) and high-resolution electric current flow maps (bottom row of Figure 3) have been simultaneously measured for the three samples.

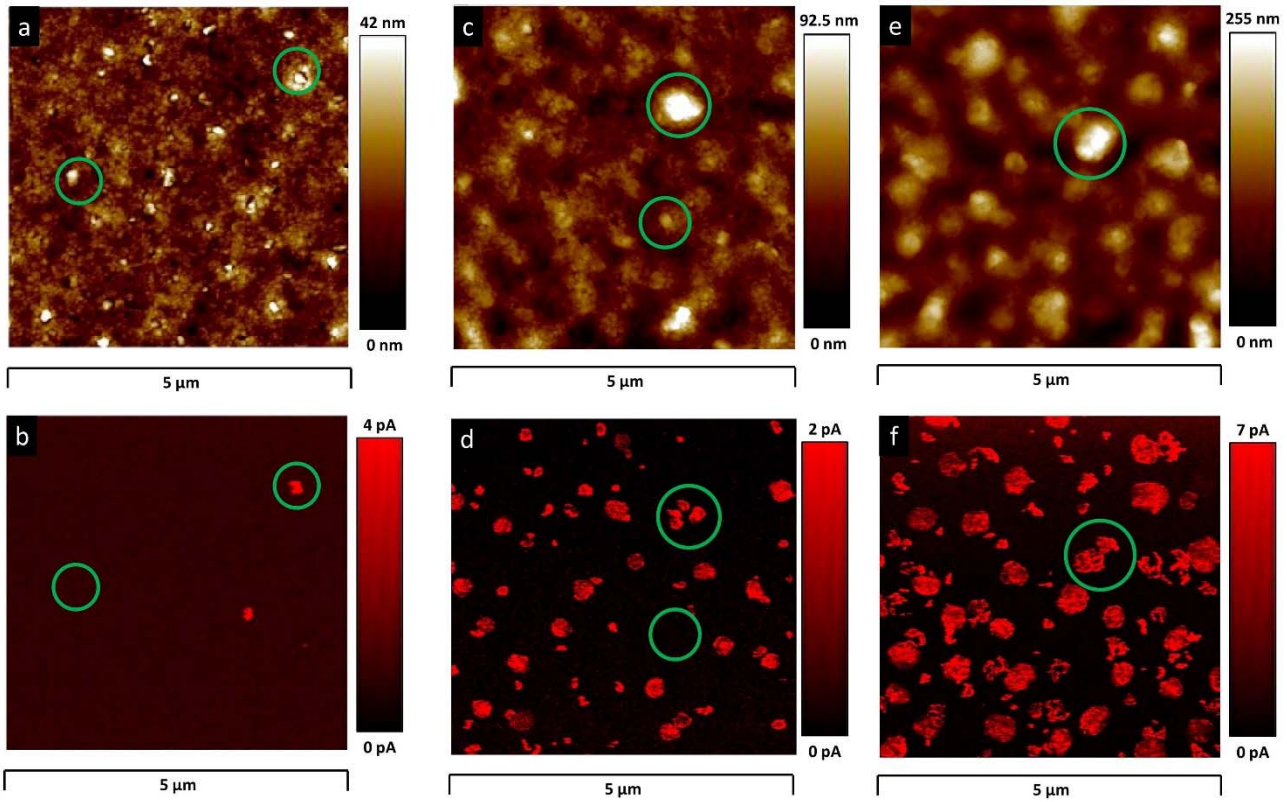

Figure 3 - *C-AFM topography images (top row) and the corresponding current flow maps (bottom row) for the 95:5 $_{wt/wt}$ (a and b, respectively), 90:10 $_{wt/wt}$ (c and d, respectively) and 80:20 $_{wt/wt}$ (e and f, respectively) P(VDF-co-TrFE):P3HT blends. The green circles designate the same morphological features in the topography and current flow images.*

In Figure 3a, the green circle on the top right side circumscribes a P3HT spike. The presence of the corresponding red spot in Figure 3b shows that this spike represents a conducting pathway from the bottom to the top of the film. On the contrary, for the P3HT domain which is inscribed in the green circle on the left side of Figure 3a no electric flow is recorded by the AFM tip, as observed in Figure 3b. This suggests that not all P3HT domains that appear at the surface are connected to the bottom electrode through conductive channels. The same observation applies for the other two loadings. However, by increasing the amount of P3HT in the blend, the number of P3HT conducting channels that traverse the film and connect the bottom and the top sides increases. Once more, there is significant polydispersity in P3HT domain size, some rough mean values being 180 nm for the 90:10 $_{wt/wt}$ blend, and 230 nm for the 80:20 $_{wt/wt}$ blend. Interestingly, the number density of continuous connecting P3HT pathways increases considerably for the higher P3HT contents. Comparing the PFM and C-AFM images for the same blend composition we see that only few conducting columns exist for the 5 wt% blend, their number density increases for the 10 wt% sample, yet it seems lower than the P3HT domains apparent in PFM, while for the 20 wt% blend, the number densities derived by PFM and C-AFM are similar. This evolution of the number density, taking into account the different depths probed by the two modalities, implies that P3HT probably tends to deplete the film/substrate interface and to segregate at the upper parts of the films. When P3HT content increases, P3HT domains grow deeper in the films, perpendicularly to the films plane.

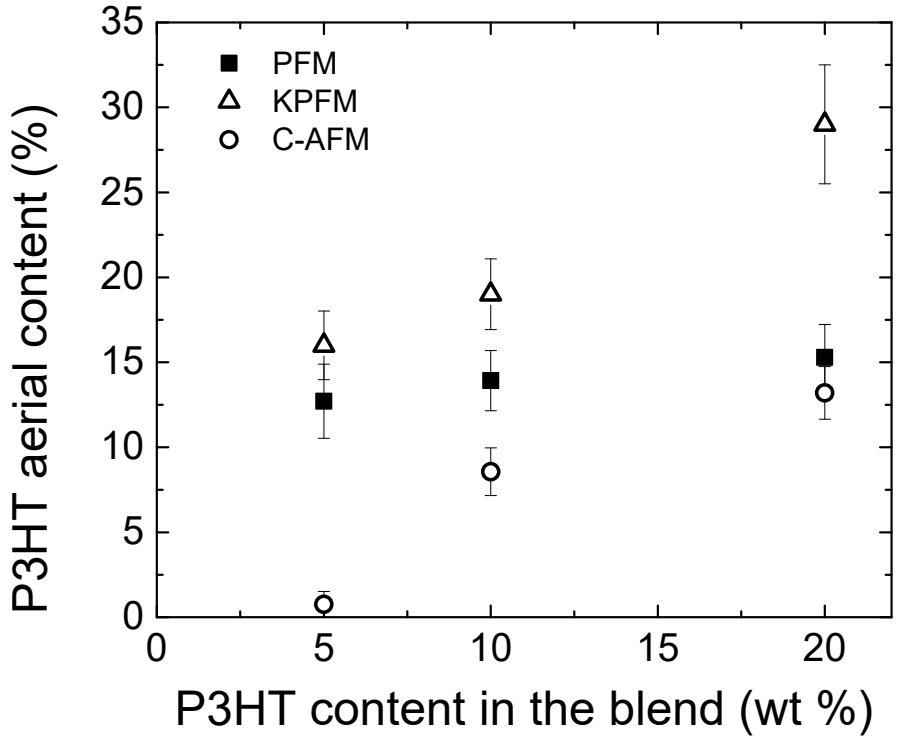

Figure 4 - *The P3HT areal content, calculated from the VPFM amplitude images, the KPFM maps and the C-FM maps for the different ferroelectric:semiconducting compositions, as a function of the respective P3HT wt% content in the blends.*

An eloquent way to confirm this outcome is provided by the plot of the areal content of P3HT, as a function of the P3HT content in the blends, presented in Figure 4, for the three modalities studied herein. The values or the areal content have been calculated by using image analysis tools (ImageJ, [29]). The error bars have been calculated by statistical analysis of five images per sample and by considering three contrast thresholds by image. Starting with the surface aerial content which is probed by PFM, we see that 12 to 15% of the surface is covered by P3HT, regardless of blends composition. Even when only 5 wt% of P3HT is added in the blend, its majority tends to segregate at the surface resulting in a surface content of 13%. This behavior of P3HT points towards a saturation limit of the blends surface composition, namely of the amount of P3HT that the surface can accommodate. We calculated the surface tensions, γ, of pure rr-P3HT and pure P(VDF-co-TrFE) films by applying the OWRK (Owens, Wendt, Rabel and Kaelble) model[18] and we have obtained the following values: γ_{P3HT} =31.85 ± 0.3 mJ m^{-2} and $\gamma_{PVDF\text{-}co\text{-}TrFE}$ = 33.02 ± 0.7 mJ m^{-2}. The slightly lower surface tension of P3HT suggests that the semiconducting polymer tends to segregate at the surface, yet, the proximity of these surface tension values and the low content of P3HT in the blends result in the saturation of the films surface composition at around 15% of P3HT.

Concerning the analysis of the KPFM images, we see that the P3HT aerial content is much higher than the actual P3HT content in the blends (for instance, 16% for the 5 wt% blend) and significantly higher than the surface content calculated on the PFM images. Recalling that KPFM probes 100 nm of the films with respect to their surface, we conclude that P3HT preferentially segregates at the upper layers of the blend films. In fact, the P3HT content at this upper layer greatly increases when the P3HT loading in the blend increases (30% of

P3HT at a 20 wt% loading). At the same time, the evolution of the aerial content of P3HT in the C-AFM images shows that the amount of P3HT that contributes to conducting pathways from the top to the bottom electrode enhances significantly with P3HT content. This implies that adding P3HT in the blend results in the expansion of P3HT domains along the vertical direction with respect to the film's plane.

Stepping back and combining the information contained in Figure 4, we propose the following scheme for the three-dimensional morphology of the P(VDF-co-TrFE):P3HT blend films and its evolution with respect to P3HT loading. At low loadings, P3HT primarily resides the surface of the film, at a surface composition that is dictated by energetics, namely by the competition of the two polymers due their respective surface energies. The rest of P3HT is primarily located at the upper layer of the film and just a very small amount reaches the interface with the substrate, resulting in very few conducting pathways. When P3HT content increases, the surface composition is practically unaffected, but the upper part of the film is further enriched with P3HT. Adding extra P3HT results in the expansion of P3HT domains along the film's z-direction, creating, thus, more conducting pathways.

Such a morphological arrangement of the two polymers in the blend could be attributed to the lower surface tension of P3HT that in principle drives this polymer towards the surface. Nonetheless, one should consider that these blend films are prepared by spin-coating which is a dynamic process that freezes the sample in a non-equilibrium state. Specifically, Heriot and Jones[30] studied the phase separation of polymer blends during spin coating and concluded that during solvent evaporation there is the formation of a layered structure (parallel to the film's plane) which subsequently breaks-up into lateral domains. In a latter publication it was demonstrated that self-stratification is also possible, depending on the evaporation rate during spin-coating[31]. The insights on the phase separation of two polymers during film formation by spin-coating provided by these reports could be related to the morphological scheme presented above for the P(VDF-co-TrFE):P3HT blend; the segregation of P3HT at the upper part of the film could be related to the formation of the layered (stratified) structure, while the increase of perpendicular P3HT domains that eventually link the two sides of the films could be related to the observed break-up in lateral domains. Although such an approach can justify the morphological features observed in the P(VDF-co-TrFE):P3HT blend, it omits a crucial parameter that is the inherent tendency of these two polymers to crystallize. Competition between crystallization, phase separation and solvent evaporation dynamics runs blend films formation quite complex. Therefore, controlling the morphology of these blend films is extremely difficult. In order to efficiently use the ferroelectric:semiconducting polymer blends in organic electronic devices, one should turn towards alternative strategies for the preparation of a well-defined structure that complies with the proposed ideal morphology. Patterning could provide realistic solutions in this respect, either by means of laser-induced patterning,[32] or by nano-imprint lithography[33].

4. Conclusions

To conclude, the combination of AFM, PFM, KPFM and C-AFM has been used to unveil qualitative information about the three-dimensional morphology of ferroelectric:semiconducting P(VDF-co-TrFE):rr-P3HT blend films. The combination of these modalities allows discriminating the two phases laterally and in-depth, in a non-destructive way. The evaluation of the recorded images and the calculation of the areal P3HT content has

revealed the saturation of the surface at 15% of P3HT and the preferential segregation of P3HT at the upper part of the film, within the first 100 nm with respect to the surface. The efficient formation of P3HT domains that traverse perpendicularly the films and create continuous conducting pathways is achieved only for the high P3HT loadings studied herein. Yet, at these high loadings KPFM exposed the existence of an interconnected P3HT network that is lying partially buried by P(VDF-co-TrFE). These results well-document that the morphology of the ferroelectric:semiconducting blends significantly deviates from the ideal morphology proposed for the efficient operation of memory devices. Furthermore, achieving the minimum lateral P3HT feature size of 5 nm that was estimated to be sufficient for charge injection and charge transport[7] in phase-separated blends seems un-realistic. Other approaches, such as patterning, should be followed.

Acknowledgements and funding information

This work was performed within the framework of the Labex AMADEus program (ANR-10-LABEX-0042-AMADEUS) with the financial support of the French State Initiative d'Excellence IdEx (ANR-10-IDEX-003-02). Financial support from the HOMERIC Industrial Chair (Arkema/ANR) with the grant agreement no AC-2013-365 is also acknowledged. The ferroelectric measurements have been conducted at the ELORPrintTec Platform (ANR-10-EQPX-28-01/Equipex ELORPrintTec).

Conflict of Interest
The authors declare that there is no conflict of interest.

References

1. Asadi K, de Leeuw DM, de Boer B, Blom PWM (2008) Organic non-volatile memories from ferroelectric phase-separated blends. Nature Materials 7 (7):547-550. doi:10.1038/nmat2207
2. Asadi K, de Boer TG, Blom PWM, de Leeuw DM (2009) Tunable Injection Barrier in Organic Resistive Switches Based on Phase-Separated Ferroelectric–Semiconductor Blends. Advanced Functional Materials 19 (19):3173-3178. doi:10.1002/adfm.200900383
3. Scott JF (2000) Ferroelectric memories today. Ferroelectrics 236 (1):247-258. doi:10.1080/00150190008016056
4. Asadi K (2020) Resistance switching in two-terminal ferroelectric-semiconductor lateral heterostructures. Applied Physics Reviews 7 (2):021307. doi:10.1063/1.5128611
5. McNeill CR, Asadi K, Watts B, Blom PWM, de Leeuw DM (2010) Structure of Phase-Separated Ferroelectric/Semiconducting Polymer Blends for Organic Non-volatile Memories. Small 6 (4):508-512. doi:10.1002/smll.200901719
6. Asadi K, Wondergem HJ, Moghaddam RS, McNeill CR, Stingelin N, Noheda B, Blom PWM, de Leeuw DM (2011) Spinodal Decomposition of Blends of Semiconducting and Ferroelectric Polymers. Advanced Functional Materials 21 (10):1887-1894. doi:10.1002/adfm.201001505
7. Ghittorelli M, Lenz T, Sharifi Dehsari H, Zhao D, Asadi K, Blom PWM, Kovács-Vajna ZM, de Leeuw DM, Torricelli F (2017) Quantum tunnelling and charge accumulation in organic ferroelectric memory diodes. Nature Communications 8 (1):15741. doi:10.1038/ncomms15841
8. Kemerink M, Asadi K, Blom PWM, de Leeuw DM (2012) The operational mechanism of ferroelectric-driven organic resistive switches. Organic Electronics 13 (1):147-152. doi:https://doi.org/10.1016/j.orgel.2011.10.013
9. Kang SJ, Park YJ, Bae I, Kim KJ, Kim H-C, Bauer S, Thomas EL, Park C (2009) Printable Ferroelectric PVDF/PMMA Blend Films with Ultralow Roughness for Low Voltage Non-Volatile Polymer Memory. Advanced Functional Materials 19 (17):2812-2818. doi:10.1002/adfm.200900589

10. Li M, Stingelin N, Michels JJ, Spijkman M-J, Asadi K, Beerends R, Biscarini F, Blom PWM, de Leeuw DM (2012) Processing and Low Voltage Switching of Organic Ferroelectric Phase-Separated Bistable Diodes. Advanced Functional Materials 22 (13):2750-2757. doi:10.1002/adfm.201102898
11. Khan MA, Bhansali US, Almadhoun MN, Odeh IN, Cha D, Alshareef HN (2014) High-Performance Ferroelectric Memory Based on Phase-Separated Films of Polymer Blends. Advanced Functional Materials 24 (10):1372-1381. doi:10.1002/adfm.201302056
12. Costa C, Nunes-Pereira J, Rodrigues LC, Silva M, Gomez Ribelles JL, Lanceros-Méndez S (2013) Novel poly(vinylidene fluoride-trifluoroethylene)/poly(ethylene oxide) blends for battery separators in lithium-ion applications. Electrochimica Acta 88:473–476. doi:10.1016/j.electacta.2012.10.098
13. Khikhlovskyi V, Wang R, van Breemen AJJM, Gelinck GH, Janssen RAJ, Kemerink M (2014) Nanoscale Organic Ferroelectric Resistive Switches. The Journal of Physical Chemistry C 118 (6):3305-3312. doi:10.1021/jp409757m
14. Khikhlovskyi V, van Breemen AJJM, Michels JJ, Janssen RAJ, Gelinck GH, Kemerink M (2015) 3D-morphology reconstruction of nanoscale phase-separation in polymer memory blends. Journal of Polymer Science Part B: Polymer Physics 53 (17):1231-1237. doi:10.1002/polb.23769
15. Su GM, Lim E, Kramer EJ, Chabinyc ML (2015) Phase Separated Morphology of Ferroelectric–Semiconductor Polymer Blends Probed by Synchrotron X-ray Methods. Macromolecules 48 (16):5861-5867. doi:10.1021/acs.macromol.5b01354
16. Pandey SS, Takashima W, Nagamatsu S, Endo T, Rikukawa M, Kaneto K (2000) Regioregularity vs Regiorandomness: Effect on Photocarrier Transport in Poly(3-hexylthiophene). Japanese Journal of Applied Physics 39 (Part 2, No. 2A):L94-L97. doi:10.1143/jjap.39.l94
17. Spampinato N, Maiz J, Portale G, Maglione M, Hadziioannou G, Pavlopoulou E (2018) Enhancing the ferroelectric performance of P(VDF-co-TrFE) through modulation of crystallinity and polymorphism. Polymer 149:66-72. doi:https://doi.org/10.1016/j.polymer.2018.06.072
18. Owens DK, Wendt RC (1969) Estimation of the surface free energy of polymers. Journal of Applied Polymer Science 13 (8):1741-1747. doi:10.1002/app.1969.070130815
19. Matavž A, Bobnar V, Malič B (2017) Tailoring Ink–Substrate Interactions via Thin Polymeric Layers for High-Resolution Printing. Langmuir 33 (43):11893-11900. doi:10.1021/acs.langmuir.7b02181
20. Lacroix C (2014) Etude des mélanges de polymères semi-conducteur / ferroélectrique en films minces : application en électronique organique.
21. Yuan Y, Reece TJ, Sharma P, Poddar S, Ducharme S, Gruverman A, Yang Y, Huang J (2011) Efficiency enhancement in organic solar cells with ferroelectric polymers. Nature Materials 10 (4):296-302. doi:10.1038/nmat2951
22. Yang B, Yuan Y, Sharma P, Poddar S, Korlacki R, Ducharme S, Gruverman A, Saraf R, Huang J (2012) Tuning the Energy Level Offset between Donor and Acceptor with Ferroelectric Dipole Layers for Increased Efficiency in Bilayer Organic Photovoltaic Cells. Advanced Materials 24 (11):1455-1460. doi:10.1002/adma.201104509
23. Gutiérrez-Fernández E, Rebollar E, Cui J, Ezquerra TA, Nogales A (2019) Morphology and Ferroelectric Properties of Semiconducting/Ferroelectric Polymer Bilayers. Macromolecules 52 (19):7396-7402. doi:10.1021/acs.macromol.9b00859
24. Mehta RR, Silverman BD, Jacobs JT (1973) Depolarization fields in thin ferroelectric films. 44 (8):3379-3385. doi:10.1063/1.1662770
25. Batra IP, Wurfel P, Silverman BD (1973) Phase Transition, Stability, and Depolarization Field in Ferroelectric Thin Films. Physical Review B 8 (7):3257-3265. doi:10.1103/PhysRevB.8.3257
26. Melitz W, Shen J, Kummel AC, Lee S (2011) Kelvin probe force microscopy and its application. Surface Science Reports 66 (1):1-27. doi:https://doi.org/10.1016/j.surfrep.2010.10.001
27. Liscio A, Palermo V, Fenwick O, Braun S, Müllen K, Fahlman M, Cacialli F, Samorí P (2011) Local Surface Potential of π-Conjugated Nanostructures by Kelvin Probe Force Microscopy: Effect of the Sampling Depth. Small 7 (5):634-639. doi:10.1002/smll.201001770
28. Brinkmann M (2011) Structure and morphology control in thin films of regioregular poly(3-hexylthiophene). 49 (17):1218-1233. doi:https://doi.org/10.1002/polb.22310
29. Schneider CA, Rasband WS, Eliceiri KW (2012) NIH Image to ImageJ: 25 years of image analysis. Nature Methods 9 (7):671-675. doi:10.1038/nmeth.2089
30. Heriot SY, Jones RAL (2005) An interfacial instability in a transient wetting layer leads to lateral phase separation in thin spin-cast polymer-blend films. Nature Materials 4 (10):782-786. doi:10.1038/nmat1476
31. Mokarian-Tabari P, Geoghegan M, Howse JR, Heriot SY, Thompson RL, Jones RAL (2010) Quantitative evaluation of evaporation rate during spin-coating of polymer blend films: Control of film structure through

defined-atmosphere solvent-casting. The European Physical Journal E 33 (4):283-289. doi:10.1140/epje/i2010-10670-7
32. Martínez-Tong DE, Rodríguez-Rodríguez Á, Nogales A, García-Gutiérrez M-C, Pérez-Murano F, Llobet J, Ezquerra TA, Rebollar E (2015) Laser Fabrication of Polymer Ferroelectric Nanostructures for Nonvolatile Organic Memory Devices. ACS Applied Materials & Interfaces 7 (35):19611-19618. doi:10.1021/acsami.5b05213
33. Nougaret L, Kassa HG, Cai R, Patois T, Nysten B, van Breemen AJJM, Gelinck GH, de Leeuw DM, Marrani A, Hu Z, Jonas AM (2014) Nanoscale Design of Multifunctional Organic Layers for Low-Power High-Density Memory Devices. ACS Nano 8 (4):3498-3505. doi:10.1021/nn406503g